Experimental and computational aeroelastic damping of an Offshore Wind Turbine on a monopile foundation

R. Shirzadeh, C. Devriendt, M.A. Bidakhvidi, P. Guillaume
Vrije Universiteit Brussel, Department of Mechanical Engineering, Acoustics and Vibration Research Group, Pleinlaan 2, 1050 Brussel, Belgium
e-mail: **rshirzad@vub.ac.be**

Abstract
In this study, Operational Modal Analysis (OMA) is used to identify the natural frequencies and damping values of the modes of an Offshore Wind Turbine (OWT) present in the response due to the stochastic excitation of ambient loads. Estimations of the aeroelastic damping of the operational turbine modes (including the effects of the aerodynamic, hydrodynamic and soil forces) give a quantitative view of the stability characteristics of the wind turbine. Two different test cases including an overspeed stop and ambient excitation have been considered. The experimental data have been obtained during a measurement campaign on an offshore wind turbine in the Belgian North Sea and the results are compared with the numerical simulations which are implemented in HAWC2.This project is in the framework of the Flemish funded offshore wind infrastructure project.

1 Introduction

The size of commercial wind turbines has increased dramatically in the last 25 years from approximately a rated power of $50kW$ and a rotor diameter of $10-15m$ up to todays commercially available $5MW$ machines with a rotor diameter of more than $120m$. This development has forced the design tools to change, from simple static calculations assuming a constant wind to dynamic simulation software that, from the unsteady aerodynamic loads, model the aeroelastic response of the entire wind turbine construction (including tower, drive train, rotor and control system). Aeroelastic tools are mainly developed at the universities and research laboratories in parallel with the evolution of commercial wind turbines. During the development of some of the early large machines, the dangers of aeroelastic instability were considered to be a real concern, and much analysis work was directed to demonstrate that individual turbine designs would not be susceptible to it. However, partly no doubt because of the high torsional rigidity of the closed cell hollow structure adopted for most wind turbine blades, aeroelastic instability has not yet been found to be critical in practice, and stability analyses are no longer regarded as an essential part of the design process. This may change, however, if designs become more flexible. Aeroelastic instability can arise when the change in aerodynamic loads resulting from a blade displacement is such as to exacerbate the displacement rather than diminish it, as is normally the case. This is very crucial to correctly estimate the damping ratios for a wind turbine as the amplitude of vibrations at resonance are inversely proportional to these ratios [1]. The overall damping of the first bending mode of an offshore wind turbine consists of a combination of aerodynamic damping, damping due to vortex shedding and damping due to constructive devices, such as a tuned mass damper, and additional damping, e.g. structural damping [2]. Compared to onshore support structures, the additional damping is further influenced by effects such as soil damping and hydrodynamic damping [3]. Analytical methods exist to estimate the aeroelastic damping for stationary and rotating wind turbines. However, experimental results are needed to verify and/or upgrade the analysis.

James et. al. [4] estimated the modal damping using strain–gauge data from an operating wind turbine. The cross–correlation (or auto–correlation) functions has been applied on strain–gauge time histories. They then used the Polyreference method to extract the modal parameters from correlation functions. The method has been verified for a vertical axis wind turbine. Hansen et. al. [5] described two different experimental methods for estimating the aeroelastic frequencies and damping of the operational modes of wind turbines from experiments. They compared the results with theoretical predictions from the stability tool HAWCStab. In this study the aeroelastic simulation of Vestas V90 3MW wind turbine is done using HAWC2 aeroelastic code which is developed at Risø DTU. The simulations are carried out for two different test cases, namely the overspeed stop test and ambient excitation, and the results are compared with the experimental data. Here we consider the first for-aft mode to extract the frequency and damping for both measurements.

2 Offshore measurements

Within this project two measurement campaigns have been planned. The first short measurement campaign focused on performing an overspeed test with the aim of obtaining a first estimate of the damping value of the fundamental for-aft vibration mode of the wind turbine. During the second long term measurement campaign we are continuously monitoring the vibration levels and the evolution of the frequencies and damping of the fundamental modes of the tower and foundation. Both the resonance frequencies and damping values are crucial to quantify the reliability and the lifetime of offshore wind turbines both in the design phase as during its life-cycle. These parameters will also be analyzed to see if they can provide indications about the current state of the soil and foundation characteristics for e.g. monitoring scour development [6]. The long term measurement campaign will last between 6 months and 1 year. The measurement campaigns are performed at the Belwind wind farm, which consists of 55 Vestas V90 3MW wind turbines. The wind farm is located in the North Sea on the Bligh Bank, $46km$ off the Belgian coast (Figure 1).

Figure 1: A render of an offshore Wind turbine at Belwind (1) location Belwind wind farm (2) park layout Belwind wind farm (3).

The hub-height of the wind turbine is on average $72m$ above sea-level. Each transition piece is $25m$ heigh and has a weight of $120ton$. The tests are performed on the BBCO1-turbine that is located in the north of the wind farm directly next to the offshore high voltage substation (OHVS). The wind turbine is placed on a monopile foundation structure with a diameter of $5m$ and a wall-thickness of $7cm$. The actual water depth at the location of BBCO1 is $22.9m$ and the monopile has a penetration depth of $20.6m$. The soil is considered stiff and mainly consists of sand. The structures instrumented in this campaign are the tower and transition piece. Measurements are taken at 4 levels on 9 locations using a total of 10 sensors. The measurement locations are indicated in Figure 2 by yellow circles. The locations are chosen based on the convenience of sensor mounting, such as the vicinity of platforms. The chosen levels are $67m$, $37m$, $23m$ and $15m$ above sea level. The interface level between the transition piece and the wind turbine is at $17m$ above sea level. There are two accelerometers mounted at the lower three levels and four at the top level. The chosen configuration is primarily aimed at identification of tower bending modes. The two extra sensors on the top level are placed to capture the tower torsion.

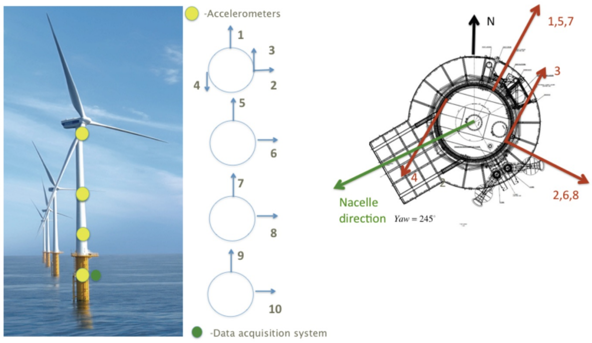

Figure 2: measurement locations on BBCO1

During the short measurement campaign, discussed in this paper, the sensors 7 and 8 were not yet installed. In order to classify the operating conditions of the wind turbine during the measurements SCADA data (power, rotor speed, pitch angel, nacelle direction) is gathered at a sample rate of $1Hz$. In order to monitor also the varying environmental conditions, the ambient data (wind speed, wind direction, significant wave height, air temperature, ...) is being collected at 10 minute intervals.

3 Simulations

This section describes the aeroelastic simulation of Vestas V90 3MW wind turbine which is mounted atop a monopile with a flexible foundation in $22.9m$ water depth. The numerical simulations have been carried out using HAWC2 aeroelastic code developed at Risø DTU. HAWC2 uses a multi-body formulation, allowing the user to model each component of the turbine as a separate body. The implementation of each body is carried out adopting a finite element theory. The code is capable to simulate the structural response of a pitch controlled horizontal axis wind turbine(HAWT) subject to aerodynamic, hydrodynamic and soil loads. In principle HAWC2 code is a code intended for calculating wind turbine response in time domain. A schematic picture consists of the foundation geometry as well as wind turbine can be seen in figure 3. The specifications of the V90-3MW offshore wind turbine are summarized in Table 1. This wind turbine is a

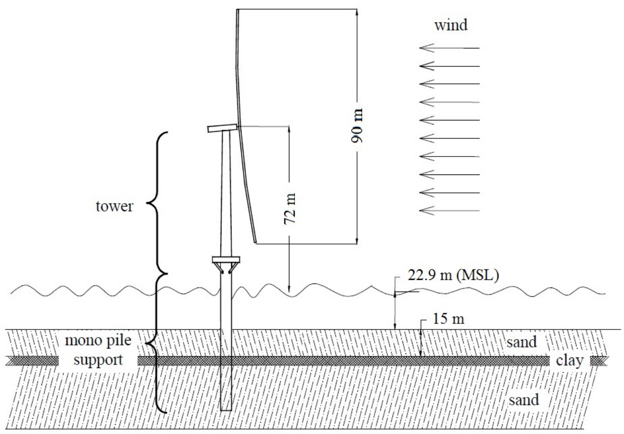

Figure 3: Schematic drawing of the wind turbine mounted on a monopile foundation

conventional three-bladed, upwind variable speed, pitch-blade controlled turbine. The detailed specifications of the blade aerodynamic properties; monopile foundation, tower, nacelle and drivetrain structural properties are provided as an input file for the HAWC2 code. The hydrodynamic and elastic properties of the offshore support are also collected. The wind inflow data and irregular wave kinematics are measured during the experiments and have been imported for the simulations. The distributed tower properties of the Vestas V90 3-MW wind turbine is based on the base diameter ($4.307m$) and thickness ($0.025m$), top diameter ($2.40m$) and thickness ($0.013m$). The thickness and radius of the tower are assumed to be linearly tapered from base to the tower top. The monopile foundation has a constant diameter ($5m$) and thickness ($0.07m$) and is extended from the bottom of the transition piece to the soil by a soil penetration length of $20.6m$. The Young's modulus and shear modulus are taken to be $210GPa$ and $80.8GPa$ respectively. Furthermore the effective density of the steel is $8500kg/m^3$ to account for paints, bolts, welds and flanges that are not accounted for in the thickness data. Because we don't have the distributed properties for the blades we scaled down the data from NREL 5MW reference wind turbine [7] to generate the input file. The overall mass, first mass moment of inertia, second mass moment of inertia, and nominal radial CM location of each blade are is $8244kg$, $1.3 \times 10^5 kg.m^2$, $3.3 \times 10^6 kg.m^2$ and $15.9m$ with respect to the blade root, respectively.

Rating	3 MW
Rotor position, Rotor type	Upwind, 3-Bladed
Control	Variable Speed, Collective Pitch
Drivetrain	High Speed, Multiple-Stage Gearbox
Rotor, Hub Diameter	$90m$, $2.32m$
Hub Height (above MSL)	$72m$
Cut-In, Rated, Cut-Out Wind Speed	$3.5m/s$, $15m/s$, $25m/s$
Cut-In, Rated, Cut-out Rotor Speed	$8.6rpm$, $16.1rpm$, $18.4rpm$
Shaft Tilt, Coning	$6°$, $4°$
Rotor Weight	$39.8ton$
Nacelle Mass	$91ton$
Tower Mass	$108ton$

Table 1: Summary of properties for the Vestas 3-MW wind turbine

The aerodynamic model in HAWC2 is based on the Blade Element Momentum theory (BEM) which is extended with models to handle the dynamic inflow, skew inflow, shear effect on induction, effect from large blade deflections and tip loss. Although two dynamic stall models namely Stig øye model and modified Beddoes-Leishmann model are included in the code. It is possible to model both deterministic and stochastic wind in HAWC2. The deterministic part of the wind includes mean wind velocity, sudden acceleration, linear trend, special gust events, and special shears. The stochastic wind usually referred as turbulent wind and is not considered in this study. Furthermore, the tower shadow effects, which accounts for the wind condition changes near the tower, are used in simulations.

The hydrodynamic loads in HAWC2 are based on the Morrisons equation. The water kinematics describes how the sea condition is considered to affect the structure. The wave kinematics are provided through a defined DLL (Dynamic Link Library) interface, including both regular and irregular airy waves. Two different empirical wave spectra namely Pierson Moskowitz (PM) and JONSWAP are implemented in HAWC2. For current analyses the PM spectra has been used which defines the distribution of energy with frequency within the sea. The significant wave height and wave period were measured during the overspeed stop test and ambient excitation and were $0.5m$ and 3.5 second. The wave direction makes an angle of $15deg$ with the direction of the nacelle.

For the pile foundation we use the distributed springs (DS) model which idealize the monopile with flexible foundation as a free-free beam with lateral(Winkler-type) springs distributed along the subsoil portion of the monopile. The beam uses the real properties of the monopile both above and below the mudline. The spring stiffness of the subsoil portion is calculated based on the *p-y* model and are depth-dependent [7]. Soil models for sand shows a relatively simple non-linear behavior. Such models are well described in certain standards and the derivation is not very complicated [8]. Based on the two soil properties effective unit weight and angle of internal friction together with the pile diameter the API standard [9] describes an easy procedure to derive the *p-y* curves over depth.

4 Results

4.1 Experimental results

As we mentioned before, two different test cases have been considered to calculate the damping and frequencies of the wind turbine. These test cases are:

- Ambient excitation which the wind speed is always very low $< 4.5m/s$ and the pitch angle is around 80.5 degrees and the rotor is slowly rotating $(0.2rpm)$. This permits us to assume that the aerodynamic damping can be neglected.
- Overspeed stop that the wind speed is the minimum required $6.5m/s$. This allows the wind turbine to speed up until $19.8rpm$. This is the speed at which the wind turbine is automatically stopped and the pitch angle is put on 88.2 degrees. So also here, we can assume that the aerodynamic damping can be neglected a few seconds after the overspeed stop took place.

An example of the measured accelerations during overspeed stop test and amibient excitation for two sensors at the highest level (1 and 2) are shown in Figure 4. A preliminary frequency domain analysis was carried out to identify the most relevant natural frequencies. For the overspeed test, the Fast Fourier Transformation (FFT) of the free decays shown in Figure 4 is calculated for all the measured time records. Before calculating the FFT, a segment is selected from the total

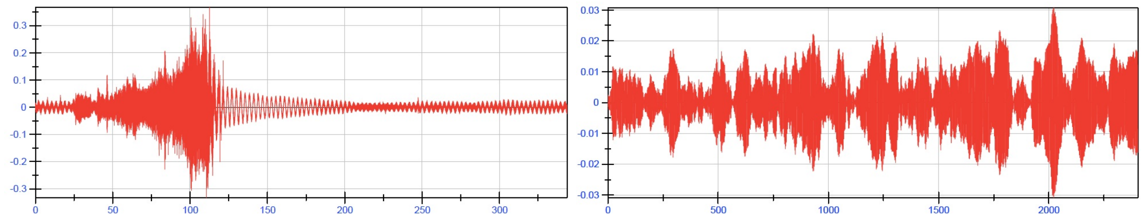

Figure 4: Measured accelerations during overspeed stop(left) and ambient excitation(right)

free decays, shown in Figure 5. For the ambient excitation test data, the Correlogram approach is used to calculate the outputs power spectrum, as shown in Figure 6. The acceleration sensor at the highest level is taken as reference response and auto and cross correlation function is calculated in a fast way using the high-speed (FFT-based) implementation. Afterwards, the PolyMAX and ML–MM [10, 11] estimators are applied to the outputs spectra calculated from both overspeed stop and ambient excitation tests.

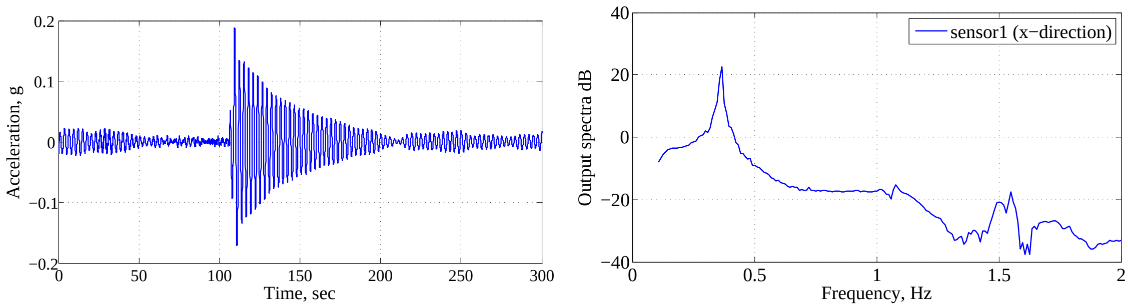

Figure 5: Overspeed stop test data processing (full time record(Left) and Calculated Outputs spectra(Right))

4.2 Simulation results

The time domain simulations are done in HAWC2 for overspeed stop test and ambient excitation to identify the dominant peaks in the frequency domain. Applying the PloyMAX and maximum likelihood estimators

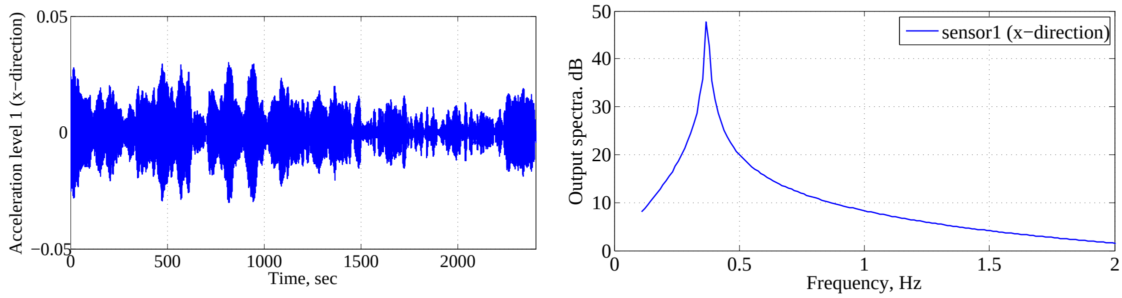

Figure 6: Ambient excitation data processing (time domain acceleration(Left) and Calculated Outputs spectra(Right))

(ML–MM) [12], the frequency and damping values can be easily calculated. In this study we are focused on the first dominant peak, which corresponds to the 1st bending mode of the tower (For-Aft mode).

4.2.1 Overspeed stop

For the overspeed stop test, the wind speed is $4m/s$ at the beginning and is increased to $6.5m/s$ in two steps. At time 60 second, the pitch angle starts to change from 0 to 88.2 degrees during an interval of 7 seconds. The thrust due to sudden collective pitch angle variation excites the tower mainly in the wind direction (For-aft mode). The top level acceleration (sensors 1) in the x direction (for-aft mode) has been plotted in Figure 7. Also the output spectra is calculated from time domain data at is shown at that figure. From output spectra different peaks are detectable. The first dominant peak occurs at frequency $0.35Hz$ is the first FA mode. Moreover, a smaller peak can be seen before the first peak around $0.28Hz$ which is related to the wave forces.

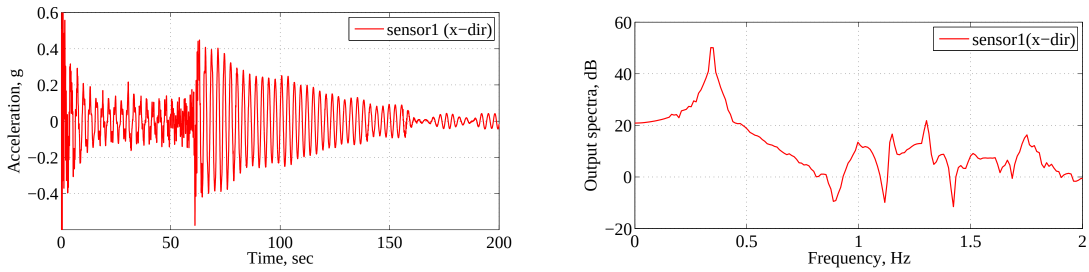

Figure 7: Overspeed stop test acceleration for sensor 1 (highest level) calculated in HAWC2(left). Calculated outputs spectra(right)

Furthermore, some peaks with higher frequencies can be seen after the first peak. These peaks correspond to the higher support structure and blade modes. The PolyMAX and ML–MM estimators are applied on stabilization chart to identify the frequencies damping ratios. Table 2 represents a comparison between simulation and experiments for the estimated resonance frequency and damping ratio of the first FA mode. This Table shows that the first FA frequency and damping calculated from both estimators compare very well with the experiments. The pre-processing parameters were chosen according to the best practice to achieve good estimates with both PolyMAX and ML–MM.

It should be noted that the effect of the wave direction in these results is noticeable. Changing this parameter can affect the damping values drastically. During the simulation, we set up the hydrodynamic calculation points and defined several parameters in the hydrodynamic module. These parameters are the inertia coefficient, C_m, the drag coefficient, C_d, and wave direction. For this study we used the default values for the C_d and C_m, which equal to 1, and set the wave direction to be $15deg$ with respect to the nacelle direction. In

	HAWC2		Experiments	
	1^{st} FA frequency, Hz	Damping ratio (%)	1^{st} FA frequency, Hz	Damping ratio (%)
PolyMAX	0.3462	1.0200	0.351	1.01
ML–MM	0.3442	1.0279	0.3523 ± 0.0001	1.08 ± 0.02

Table 2: Overspeed stop test comparison between simulation and experimental results for estimated natural frequency and damping ratio for the 1^{st} FA mode

the soil module the soil damping coefficient (k factor damping) was chosen 0.01 for this study. These are the parameters that might need to be updated when comparing with long term measurements.

4.2.2 Ambient excitation

Ambient vibration tests have the advantage of being practical and economical, as they use the freely available ambient wind excitation together with the wave excitation. Furthermore, the data is collected during the normal use of the structure and consequently the identified modal parameters are associated with realistic vibration levels. For the ambient excitation, the wind speed is $4.5m/s$ and the blade pitch angle is set to 80.5 degrees from the beginning of the simulation. The simulation is performed for an interval of $600s$ and the same data has been gathered during the simulation. The rotor speed at the beginning is $4.5rpm$ and quickly drops to $0.2rpm$ after 30 seconds. The wind and wave are assumed to be in the direction of the nacelle.

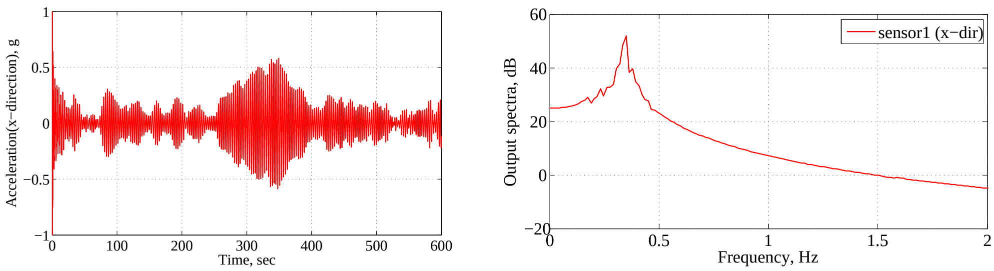

Figure 8: Ambient excitation acceleration for sensor 1 (highest level) calculated in HAWC2(left). Calculated outputs spectra(right)

The acceleration for sensor 1 in x direction (for-aft mode) during simulations and its corresponding power spectra are represented in Figure 8. We noticed that both the PolyMAX and ML–MM estimators; when applied to the outputs power spectra due to ambient excitation; are able to identify a stable mode at the vicinity of the dominant peak around $0.35Hz$ (1^{st} FA mode) similar to the overspeed stop test case. For the analysis the full time simulation is considered and the same analysis is done to estimate the modal frequency and damping of the FA mode. Table 4 shows these data compared with the results from measurements.

	HAWC2		Experiments	
	1^{st} FA frequency, Hz	Damping ratio (%)	1^{st} FA frequency, Hz	Damping ratio (%)
PolyMAX	0.3448	1.0321	0.3565	1.01
ML–MM	0.3519	1.0137	0.3565 ± 0.0001	1.08 ± 0.02

Table 3: Ambient excitation comparison between simulation and experimental results for estimated natural frequency and damping ratio for the 1^{st} FA mode

4.3 Full-System natural frequencies

A full system eigenvalue analysis performed to calculate the natural frequencies of the offshore wind turbine mounted on a foundation. The structure assumed to be flexible for all components and the results are compared with the measurements. Figure 9 represents a comparison between the measurements and simulations obtained using HAWC2 for the lowest 8 natural frequencies.

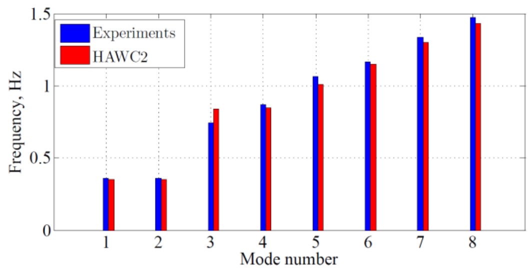

Mode	Frequency, (HAWC2)	Description
1	0.35	1st support structure fore-aft
2	0.35	1st support structure side-to-side
3	0.84	1st blade asymmetric flapwise pitch
4	0.85	1st blade asymmetric flapwise yaw
5	1.01	1st drivetrain torsion
6	1.15	2nd support structure fore-aft
7	1.3	1st blade asymmetric edgewise pitch
8	1.43	1st blade asymmetric edgewise yaw

Figure 9: Experimental and computational natural frequency comparison for 8 lowest frequencies

The designations of ”pitch” and ”yaw” in the asymmetric flapwise and edgewise blade modes stand for coupling of the blade motions with the nacelle-pitching and nacelle-yawing motions respectively. One can easily conclude that the eigenvalue-analysis is in good agreement with the experiments even for higher frequencies. However the difference is perceptible especially for higher modes which correspond to the higher tower and blade modes.

5 Conclusions and future work

The overspeed stop test and ambient excitation have been considered to estimate the first for-aft mode frequency and damping of the support structure. The structural properties of Vestas V90 3MW wind turbine as well as the wave kinematics, wind condition and soil stiffness parameters are implemented in HAWC2. The results are processed applying PolyMAX and ML–MM estimators that have been used in processing the experimental data. The comparison between the simulation results and experimental data confirms the accuracy of the simulations. Moreover a full eigenvalue analysis performed for overspeed stop test and the resonant frequencies are obtained for various modes. Comparing with the measurements, a good accuracy is seen for the lowest 10 frequencies. This ensures us to implement the further simulations for variant wind and structure conditions. In the other hand, the availability and accessibility of the computational tools can facilitate the analysis and processing the data from measurements and assist to achieve better understanding of the problem.

For future works, a detailed investigation of the effects of the pitch and yaw motions of the nacelle on the frequency and damping values should be considered. Also several simulations can be executed for different wind speeds and, wind wave directions and different wind turbine conditions to analyze the results with available methods. Furthermore, as mentioned in the simulation section, the wave kinematic e.g. direction, drag coefficient and wave spectra, can significantly affect the damping values and therefore a more detailed analysis and comparison with long term measurement data is required. This will enable us to have a better understanding of the aeroelastic damping values and consequently the fatigue life of the wind turbine.

Acknowledgements

This research has been performed in the framework of the Offshore Infrastructure Project (**http://www.owi-lab.be.org**). The short-term measurement tests were initiated by the engineers of NorthWind NV. They also supplied all relevant operational and structural data which has been used for the analysis. The authors also gratefully thank the people of Belwind NV for their support before, during and after installation of the measurement equipment.

References

[1] Devriendt C., El-Kafafy M., De Sitter G., Guillaume P., *Estimating Damping of an offshore wind turbine using an overspeed stop and ambient excitation*, in Proceeding of the 15th International Conference on Experimental Mechanics, ICEM15, Porto, Portugal.

[2] Dwight Davis. Dr. Martin Pollack. Brian Petersen, *Evaluate the Effect of Turbine Period of Vibration Requirements on. Structural Design Parameters, Technical report of findings*, Report Number: M10PC00066, Applied Physical Sciences Corp., 2010.

[3] http://www.marin.nl/web/Events/Events-2010/

[4] James G. H., Carne T. G., Veers P. S., *Damping measurements using operational data*, ASME Journal of Solar Energy Engineering 1996; 118: 190193.

[5] Hansen M.H., Thomsen K., Fuglsang P., Knudsen T., *Two methods for estimating aeroelastic damping of operational wind turbine modes from experiments*, Wind Energy, Vol. 9, 179–191, 2006.

[6] Zaaijer, M.B., Tempel, J.V.D., *Scour protection: a necessity or a waste of money?*, Proceedings of the 43 IEA Topixal Expert Meeting, 43–51, 2004.

[7] Jonkman J., Butterfield S., Musial W., Scott G., *Definition of a 5-MW Reference Wind Turbine for Offshore System Development*, NREL/TP-500-38060 National Renewable Energy Laboratory.

[8] Passon P., *Memorandum: derivation and description of the Soil-Pile-Interaction models*, IEA-Annex XXIII subtask 2, Endowed chair of Wind energy, University of Stuttgart, 2006.

[9] American Petroleum Institude; *Recommended practice for planning, describing and constructing fixed offshore platforms working stress design*, API recommended practice 2A–WSD (RP 2A–WSD) twenty–first edition, December 2000.

[10] Elkafafy M., Gauillaume P., Peeters B., Marra F., Coppotelli G., *Advanced frequency domain modal analysis for dealing with measurment noise and parameter uncertainty*, In Proceeding of IMAC-XXX, Jacksonville, FL, USA, 2012.

[11] Elkafafy M., Guillaume P., De Troyer T., Peeters B., *A frequency-Domain Maximum Likelihood Implementation using the modal model formulation*, In Proceeding of the 16th IFAC Symposium on Sytem Identification, Brussels, 2012.

[12] Guillaume P., Verboven, Vanlanduit S., *Frequency-domain maximum likelihood identification of modal parameters with confidence intervals*, In Proceedings of the 23rd International Seminar on Modal Analysis , Leuven, Belgium, 1998.